

# HIGH POWER TEST RESULTS FOR A CYLINDRICAL-SHELL SIC Higher-Order-Mode DAMPER

W. Xu

February 2024

Electron-Ion Collider  
**Brookhaven National Laboratory**

**U.S. Department of Energy**  
USDOE Office of Science (SC), Nuclear Physics (NP)

Notice: This technical note has been authored by employees of Brookhaven Science Associates, LLC under Contract No. DE-SC0012704 with the U.S. Department of Energy. The publisher by accepting the technical note for publication acknowledges that the United States Government retains a non-exclusive, paid-up, irrevocable, world-wide license to publish or reproduce the published form of this technical note, or allow others to do so, for United States Government purposes.

## **DISCLAIMER**

This report was prepared as an account of work sponsored by an agency of the United States Government. Neither the United States Government nor any agency thereof, nor any of their employees, nor any of their contractors, subcontractors, or their employees, makes any warranty, express or implied, or assumes any legal liability or responsibility for the accuracy, completeness, or any third party's use or the results of such use of any information, apparatus, product, or process disclosed, or represents that its use would not infringe privately owned rights. Reference herein to any specific commercial product, process, or service by trade name, trademark, manufacturer, or otherwise, does not necessarily constitute or imply its endorsement, recommendation, or favoring by the United States Government or any agency thereof or its contractors or subcontractors. The views and opinions of authors expressed herein do not necessarily state or reflect those of the United States Government or any agency thereof.

# HIGH POWER TEST RESULTS FOR A CYLINDRICAL-SHELL SiC Higher-Order-Mode DAMPER

Wencan Xu<sup>†,1</sup>, Z.A. Conway<sup>1</sup>, E. Daly<sup>2</sup>, J. Guo<sup>2</sup>, K. Hernandez<sup>1</sup>, D. Holmes<sup>1</sup>, R.A. Rimmer<sup>2</sup>, F. Severino<sup>1</sup>,  
K. Smith<sup>1</sup>, D. Weiss<sup>1</sup>, A. Zaltsman<sup>1</sup>

*1) Brookhaven National Laboratory, Upton, NY, 11973-5000, USA*

*2) Thomas Jefferson National Accelerator Facility, Newport News, VA, 23606, USA*

The next high-current Electron Ion Collider (EIC) is a new accelerator to be built at Brookhaven National Laboratory (BNL) in collaboration with Thomas Jefferson National Accelerator Facility (TJNAF). In the EIC Electron Storage Ring (ESR), there will be beam currents up to 2.5 A, which will excite massive Higher-Order-Modes (HOM) power in the 17 single-cell 591 MHz Superconducting Radio Frequency (SRF) cavities. To damp the HOM power in the ESR SRF cavities is a challenge. A room temperature cylindrical shell shape Silicon Carbide (SiC) Beamline HOM Absorber (BLA) was chosen as the baseline design, due to its broadband and high-power capability, and previous demonstrations at other accelerator facilities, albeit at much lower power. Because the EIC BLA HOM power dissipation is significantly greater than the previous applications, it is imperative to carry out high power testing to determine the maximum device performance levels achievable for thermal transport, RF breakdown, and mechanical stress, prior to finalizing the design. A SiC HOM absorber with state-of-the-art geometry size was prototyped to verify shrink-fit technique, test outgassing rate, and high power handling capability. This paper presents the HOM damper's prototyping and test results.

## I. Introduction

The EIC[1] will be a discovery machine, providing answers to long-elusive mysteries of matter related to our understanding of the origin of mass, structure, and binding of atomic nuclei that make up the entire visible universe. The machine will be built upon the existing Relativistic Heavy Ion Collider [2] (RHIC) at BNL, upgrading the hadron ring and adding two new Electron Rings, the ESR and the Rapid Cycling Synchrotron (RCS). Figure 1 shows, geographically, the RF systems in the EIC. In the EIC ESR, there will be 17 single-cell 591 MHz SRF cavities to compensate for up to 10 MW of synchrotronic radiation loss in the EIC ESR. The beam current, bunch length, cavity voltage, and HOM power for different operation scenarios in EIC ESR are listed in Table 1. The most challenging scenario for HOM damping is to the 72.7 kW HOM power in the 10 GeV case, which has the shortest bunch length and highest beam current. Therefore, the 10 GeV case is the focus of the HOM damper design.

The EIC SiC HOM damper will use a cylindrical shell shape, which is similar to the applications in KEKB [3], APS-U [4], Cornell [5], and TRIUMF [6]. These solid cylindrical shell shape SiC HOM dampers are based on the shrink-fit technique and use water-cooling jackets to remove the heat energy. The failure limit of the HOM absorber's power handling capability is determined by the absorber assembly's thermal transport properties and the temperature profile for the given geometry. Therefore, we will use the HOM absorbing power flux to determine the SiC HOM absorber's maximum power handling capability. The power flux (W/mm<sup>2</sup>) is defined as follows:

$$\text{Power flux} = \frac{\text{Total RF power dissipation in the absorber volume}}{\text{RF surface area of the SiC absorber}}$$

The power flux will provide design guidance for future BLAs. Previous SiC HOM damper testing [4,7] found a power flux up to 0.2 W/mm<sup>2</sup> to be tolerable, however, there is no credible data on the maximum power flux of a SiC BLA. This is the motivation of the experimental work presented in this paper.

To verify that the fabrication tolerances required for a large geometry size BLA can be met, a state-of-the-art geometry size (inner diameter: 308 mm, length 240 mm, thickness: 14 mm) BLA prototype was successfully manufactured. This prototype size is much larger than the actual BLA size needed for ESR SRF cavity (see Table 2). The maximum absorbing power flux tested on this larger BLA will provide a conservative criterion for the ESR SRF cavity HOM damper design.

---

<sup>†</sup> wxu@bnl.gov

This paper is organized as follows. Section II will describe the HOM damper design for the EIC ESR SRF cavity. Section III will present the manufacturing process and outgassing test result. In Section IV, the high power test setup and results will be discussed. Section V will present the summary and the next steps.

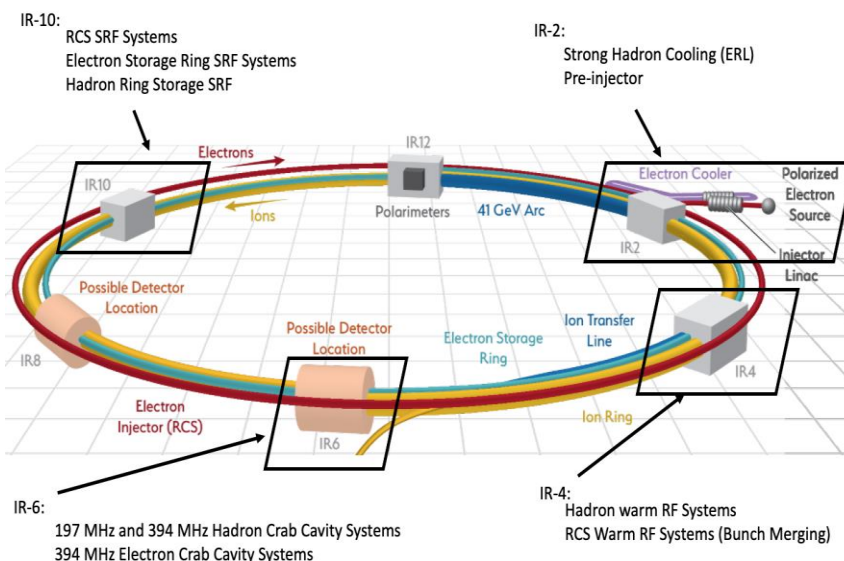


Figure 1. RF systems in EIC.

Table 1. EIC ESR operation scenarios

| Beam parameters                 | Scenarios #1 | Scenarios #2 | Scenarios #3 |
|---------------------------------|--------------|--------------|--------------|
| Beam energy (GeV)               | 5            | 10           | 18           |
| Beam current (A)                | 2.5          | 2.5          | 0.227        |
| Bunch Charge (nC)               | 27.6         | 27.6         | 10           |
| RMS Bunch length (mm)           | 9.6          | 7.7          | 8.7          |
| Number of bunches               | 1160         | 1160         | 290          |
| Cavity voltage (MV)             | 0.57         | 1.27         | 3.62         |
| Total HOM power per cavity (kW) | 65.1         | 72.7         | 2.4          |

## II. HOM damper design for EIC ESR SRF cavity

The EIC ESR SRF cavity [8, 9] is a nonsymmetrical single-cell SRF cavity design with a large beampipe and a small beampipe. Each ESR SRF cavity uses two room temperature beamline absorbers (BLAs) to damp the HOMs, one large BLA (LBLA) on the large beampipe and one small BLA (SBLA) on the small beampipe. Figure 2 shows the HOM power flow for the cavity with a 120 mm length SBLA (SBLA #1 in Table 2). The LBLA and SBLA dimensions are shown in Table 2, where two lengths of the SBLA are listed for power flux comparison. The ESR SRF cavities are laid out next to each other as shown in Figure 3, so it is reasonable to assume that the LBLA will absorb the HOM power leaked to the LBLA from both sides of the cavities. Therefore, in the case shown in Figure 2, the real absorbing power for the LBLA is 34.4 kW, while the SBLA's absorbing power is 26.5 kW. When a SiC HOM absorber is placed near a SRF cavity, it will absorb all the HOM power generated in the cavities. In addition, because of the impedance discontinuity introduced by the HOM absorber (the BLA by itself is like a pill box there), RF modes will be generated inside the BLA when a bunch is passing through. Thus, the BLA will also absorb the HOM power generated inside the BLA itself, which is called BLA self-heating. For example, the 120 mm long SBLA (SBLA #1 in

Table 2) has up to 15 kW of RF power generated inside. The longer the BLA, the more power generated inside. However, when we double the length of the SBLA (SBLA #2 in Table 2), the total power increases only by ~50% due to the cavity's HOM power not changing with the varied length of the BLA. Thus, doubling the length of the SBLA dramatically reduces the power flux from 0.47 to 0.34 W/mm<sup>2</sup>, as shown in Table 2. For the EIC ESR SRF cavity, 240 mm length for the SBLA was chosen.

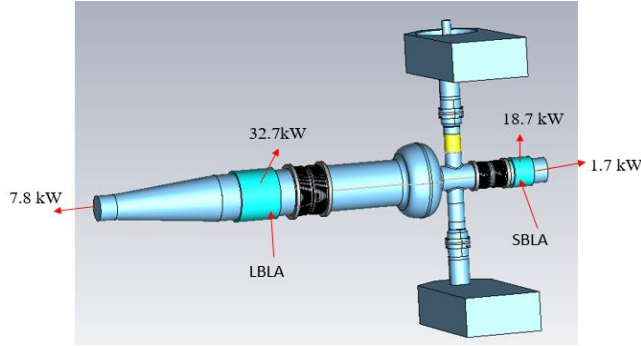


Figure 2. HOM power flow in EIC ESR SRF cavity (SBLA length: 120 mm).

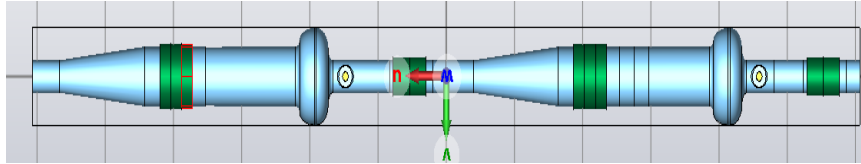


Figure 3. EIC ESR SRF cavities layout.

Table 2. HOM power absorbing in BLAs (compare lengths of SBLA)

|                                 | LBLA | SBLA #1 | SBLA #2 |
|---------------------------------|------|---------|---------|
| Radius (mm)                     | 137  | 75      | 75      |
| Length (mm)                     | 240  | 120     | 240     |
| HOM power (kW)                  | 34.4 | 26.5    | 38.3    |
| Power flux (W/mm <sup>2</sup> ) | 0.19 | 0.47    | 0.34    |

### III. SiC BLA manufacture and outgassing test

#### A. Manufacturer procedure

The manufacturing process of the SiC HOM damper is illustrated in Figure 4. A SiC housing assembly, as shown in Figure 4 (top), was brazed together from two flanges, one copper cylinder with water cooling channel on it and a stainless-steel housing. The SiC housing assembly was heated up to 145 °C in an air oven, with estimated diametral expansion to be about 0.7 mm. The SiC housing was then removed from the oven and the SiC cylinder was inserted into the housing, which is shown in Figure 4 (bottom). A photo of the final BLA assembly is shown in Figure 5.

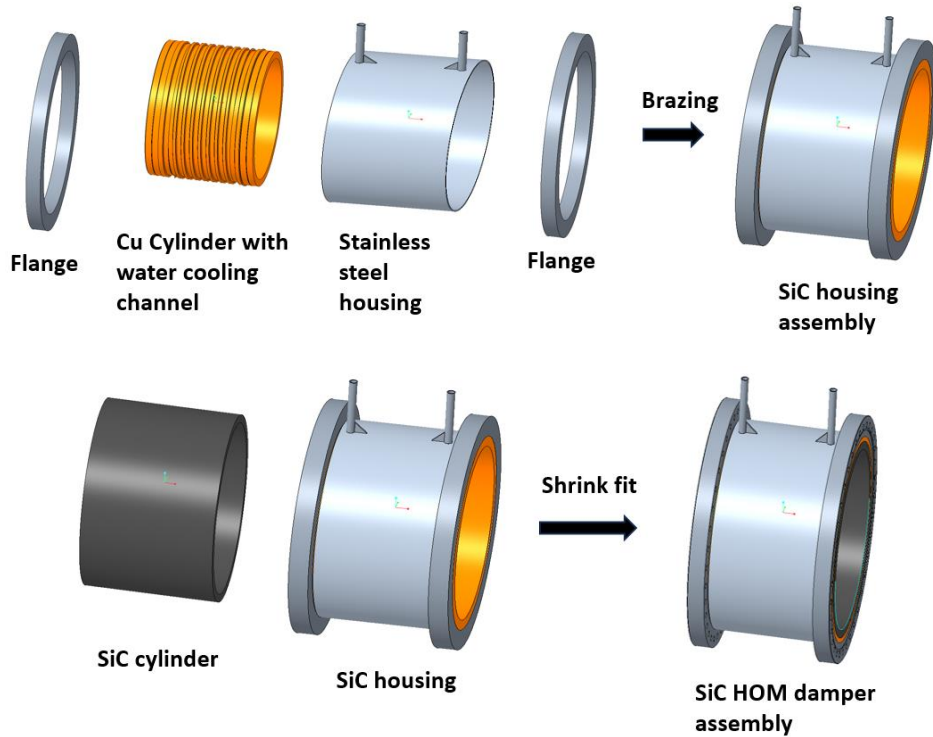


Figure 4. SiC HOM damper manufacturer process.

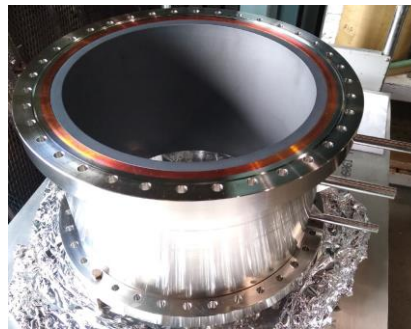


Figure 5. Shrink-fitted SiC HOM absorber assembly.

#### B. Outgassing test

Prior to the high-power RF testing, outgassing test was carried out to measure the outgassing rate of the HOM absorber assembly. This is important because the shrink-fit process may trap air between the SiC and the copper cylinder, causing the HOM absorber to act as a virtual leak. Figure 6 shows the outgassing test setup (top) and model (bottom). The system was baked at 200 °C for 96 hours. The outgassing rate was measured to be  $2.2E-10$  Torr-Liters/sec-cm<sup>2</sup>, which satisfies the high vacuum need for the ESR SRF cavity. It is worthwhile to mention that the surface finish wasn't specified when the SiC was ordered for this test. The surface finish was about Roughness Average (Ra) 3.2  $\mu$ m. For the EIC SRF cavities' HOM damper, the surface finish for both copper and SiC will be specified to be Ra 0.8  $\mu$ m, which would further lower the outgassing rate.

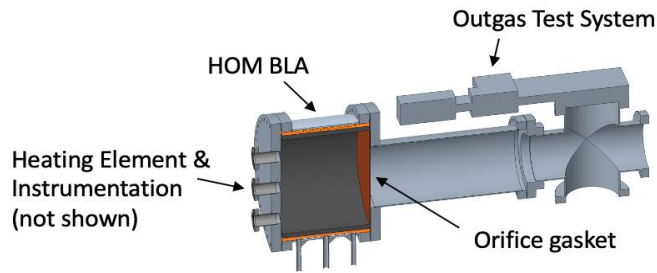
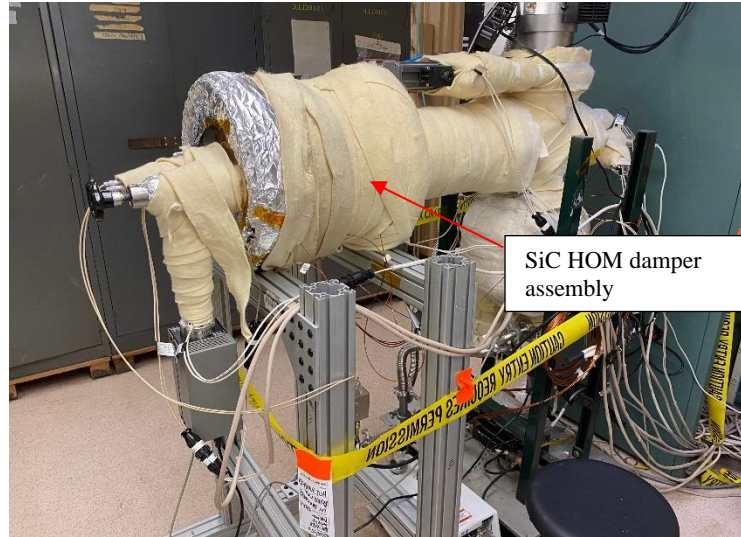


Figure 6. Outgassing test setup (top) and model(bottom).

## IV. High power RF Test

### A. High power RF test setup

The high-power test setup for SiC HOM damper is shown in Figure 7. The high-power test was carried out in the air. RF breakdown voltage in the air is much lower than in the high vacuum environment, which could potentially be a limiting factor for the thermal stress test. Should that be the case, the test setup will be improved to mitigate such an issue. RF power provided by a 704 MHz 1 MW CW klystron is delivered to the BLA with WR 1500 waveguides. Two low insertion loss ( $\sim 0.06$  dB) transitions make connections between the WR 1500 waveguide and the SiC HOM BLA. There is a directional coupler in the downstream and upstream of the SiC HOM damper. A high-power RF phase shifter is placed before the shorting plate to adjust the RF field in the BLA for balancing the RF heating along the BLA axial direction, which is determined by the temperature profiles on the BLA flanges. On the SiC HOM damper flanges, there are 6 Resistance Temperature Detector (RTD) sensors attached to each flange and each of them is 60 degrees apart. Figure 8 shows the instrumentations for the high-power test. The blue RTDs (#21, 23, 25, 27, 29, 31) are on the upstream flange while the orange RTDs (#22, 24, 26, 28, 30, 32) are on the downstream flange. There are three arc detectors near the HOM absorber: one on each transition and one on the shorting plate, as shown in Figure 8. Also, as shown in Figure 9 (left), there is an Infrared Radiation (IR) camera located on the shorting plate looking into the left side of the SiC surface while a IR detector is pointed to the opposite side of the SiC surface. Figure 9 (right) shows a typical IR camera photo when RF is on. The hottest area is the SiC surface. The temperatures measured by IR detector and IR camera are consistent with each other.

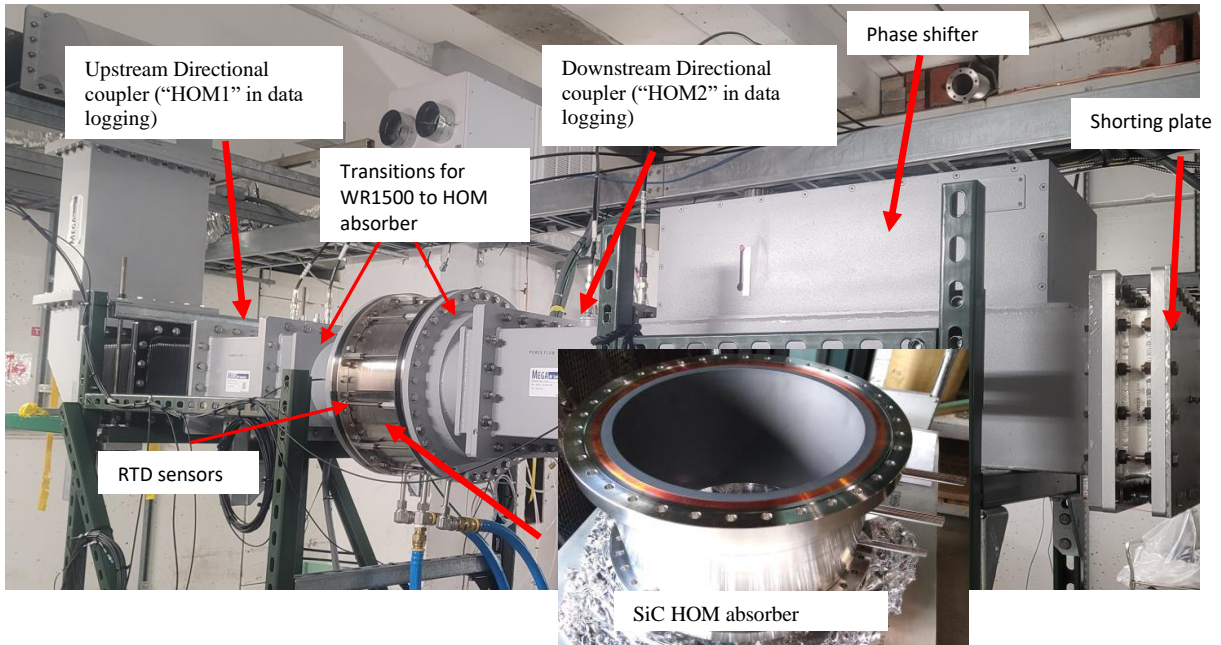


Figure 7. High Power HOM damper test setup

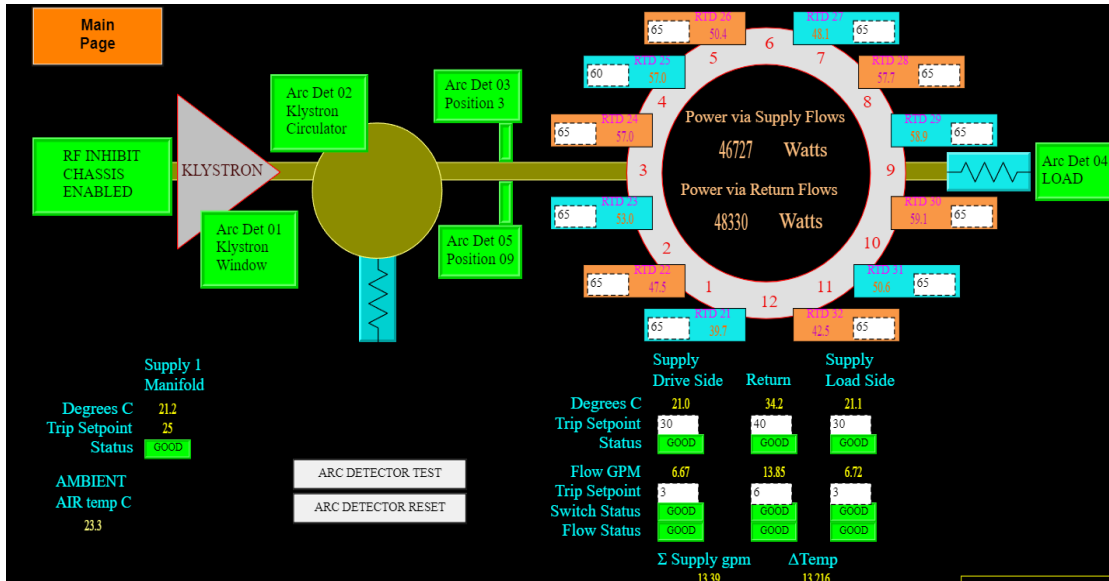


Figure 8. Instrumentation diagram for the HOM damper test



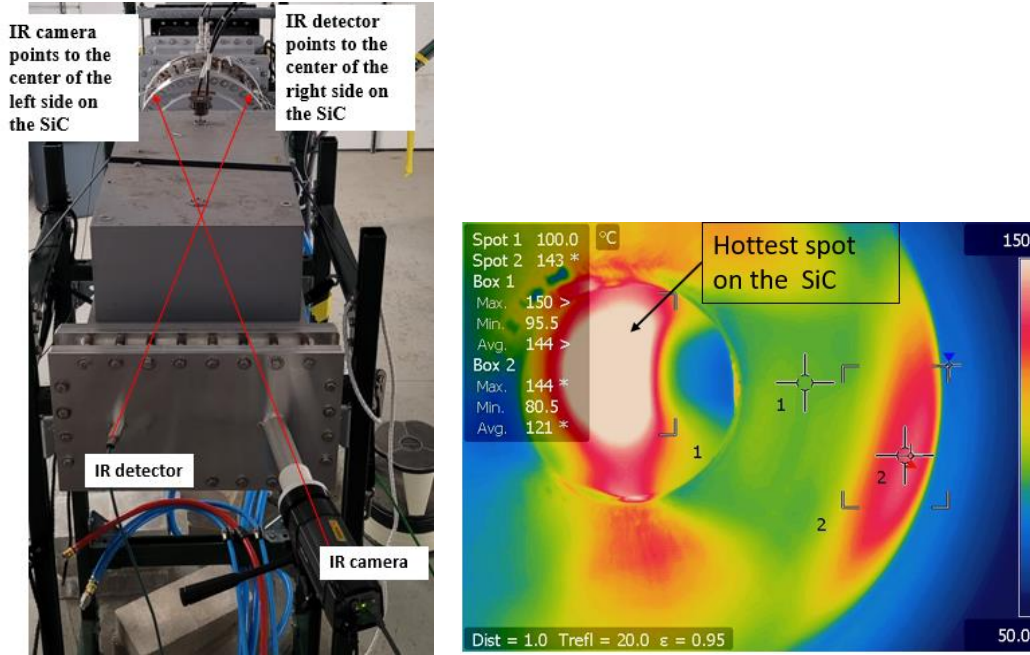


Figure 9. Left: IR camera and detector, right: Typical IR camera when RF power is on.

### B. High power test results

It is noticeable that the fundamental transverse mode (TE<sub>10</sub>) propagates in the WR1500 waveguide, and it transitions to TE<sub>10</sub> mode in the cylindrical SiC HOM damper. Thus, RF heating in the horizontal plane (the narrow side of rectangular waveguide) is much stronger than the vertical plane (the wide side of the rectangular waveguide). Therefore, the thermal stress in the test is much worse than what is expected in the case for EIC ESR SRF cavity. This is because the RF heating caused by axial symmetrical longitudinal modes will be uniform on the SiC HOM damper surface. So, the results from this test are conservative, in terms of the thermal stress caused by RF heating.

The absorbing power is measured in two ways. The first way is to use the water flow and water temperature rise. The water flow inlet and outlet have about < 2% of discrepancy due to reading error in the water flow switch, which causes less than 2% of error in the absorbing power calculation. A typical example of power data is shown in Figure 10. As shown in Figure 10 (bottom), the power fluctuation calculated via outlet flow (red curve) is larger than the power fluctuation calculated via inlet (black curve). This is because the cooling channel has two inlets and one outlet. Therefore, the outlet channel has accumulated errors. The absorbing power is calculated by averaging the measured power from inlet and outlet flow, which is 100.7 kW.

The other way to get the absorbing power is by RF power measurement in the directional couplers, with the consideration of insertion loss in the transition (~ 0.06 dB) and power loss on the waveguide. The formula for the absorbing power calculation is written as follows:

$$P_{\text{absorbing}} = (P_{\text{HOM1Forward}} - P_{\text{HOM2Forward}}) + (P_{\text{HOM2Reflect}} - P_{\text{HOM1Reflect}}) - 4 \times P_{\text{transition\_loss}} - 2 \times P_{\text{directionalcoupler\_loss}}$$

Table 3. RF Power summary

| Power                    | Result (W) |
|--------------------------|------------|
| HOM1Foward               | 418,352    |
| HOM1Reflect              | 241,683    |
| HOM2Forward              | 301,525    |
| HOM2Reflect              | 272,814    |
| Transition Loss          | 5,852      |
| Directional Coupler loss | 9,723      |

Note that the “HOM1” meant the upstream directional coupler and “HOM2” meant the downstream directional coupler (see Figure 7). Using the directional coupler measurement data shown in Figure 10 (Top), the transition loss (0.06 dB

of insertion loss) is 5.852 kW for each RF passage. The RF loss in the two directional coupler is scaled from the RF loss between the downstream directional coupler and shorting plate ( $P_{\text{HOM2Forward}} - P_{\text{HOM2Reflect}}$ ) and the distance is 0.9 meter, which turns out to be 31.9 kW/m. So, the loss in the 12 inches long directional coupler is 9.723 kW for each RF passage. The RF power used for absorbing power calculation is summarized in Table 3. Therefore, the RF dissipation in the HOM absorber is 105.1 kW. Taking the average of RF absorbing calculated by both ways, we conclude that the RF absorbing power is (102.9 $\pm$  2.2) kW. With 102.9 kW of absorbing power, the average power flux over the RF surface is 0.44 W/mm<sup>2</sup>, and the error is  $\pm$  2.1 %.

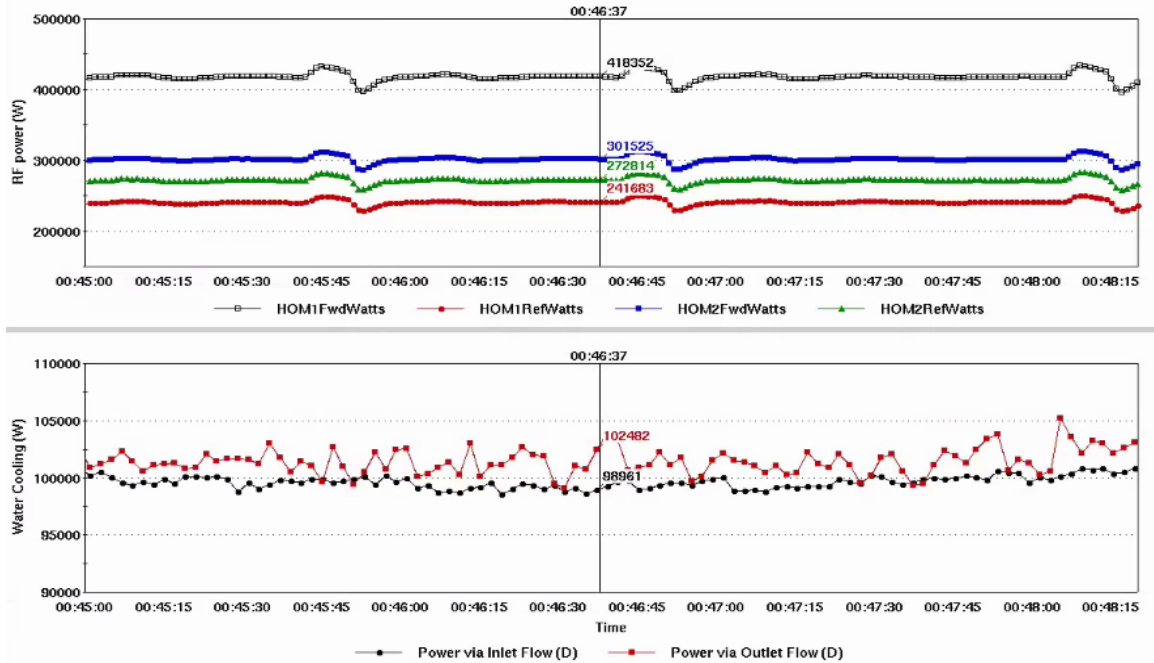


Figure 10. Example HOM test data logging.

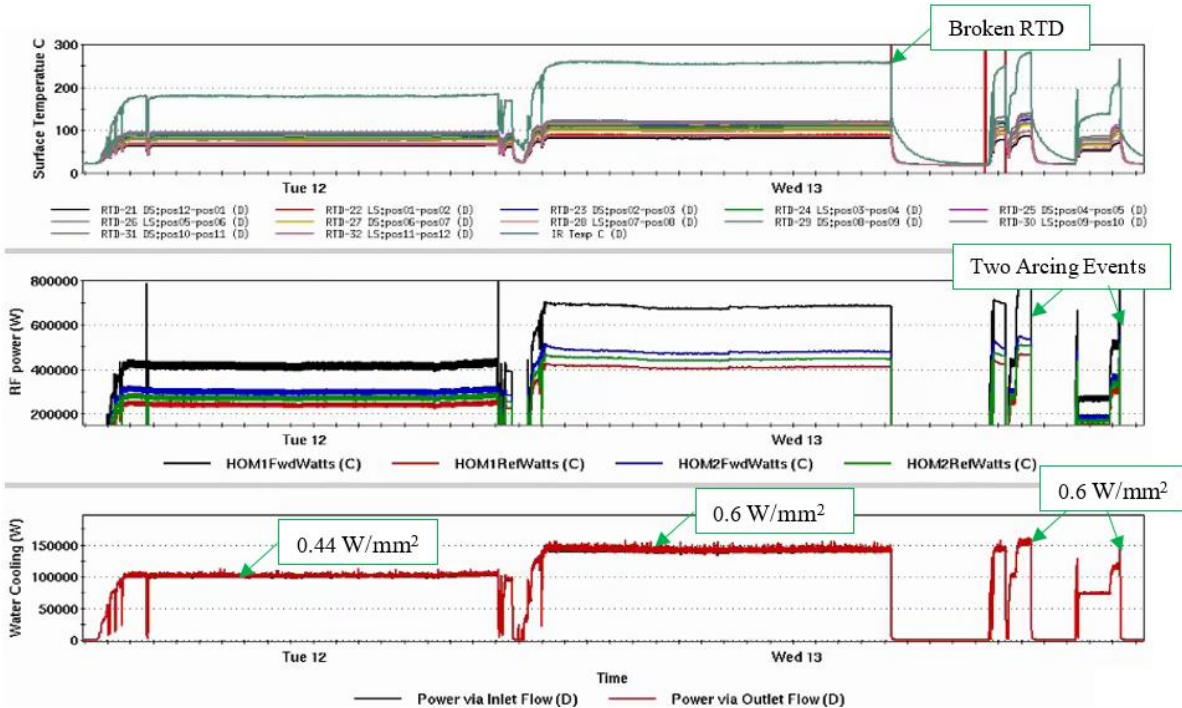


Figure 11. High power test.

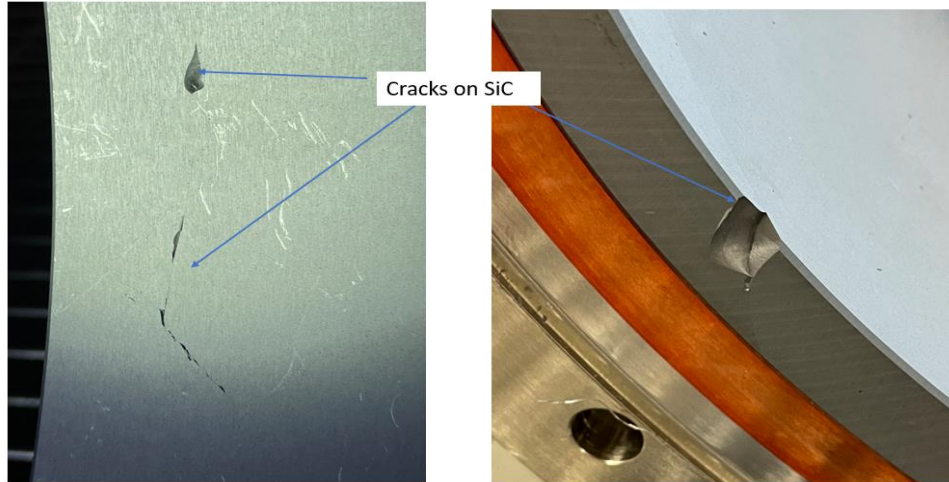


Figure 12. Crack found inside the SiC (left) and on the edge (right).

The high-power RF test was carried out in CW mode and the power was raised slowly by observing the thermal signals measured by RTDs. The RF was left on overnight ( $> 15$  hours) at multiple power flux levels: 0.1, 0.2, 0.3, 0.4, 0.5, 0.6  $\text{W}/\text{mm}^2$ . On the way up in RF power, the HOM absorber was taken apart to be inspected when the power flux reached  $0.44 \text{ W}/\text{mm}^2$  and no sign of damage was found. The RF power continued to rise until two arcing events happened at a power flux of  $0.65 \text{ W}/\text{mm}^2$ . Figure 11 shows the temperature, RF power and water-cooling power for the last two days. Nothing abnormal can be seen from the RF and temperature signals. Additionally, the IR camera didn't show any differences before and after arcing as well. After the second arcing, the HOM absorber was taken apart and damage on the SiC was found. Figure 12 shows the cracks found in the SiC surface after two arcing events. Cracks were found both inside the SiC (see Figure 12 (left)) and on the edge (see Figure 12 (right)). As there was not a singular thermal stress point in the cylindrical SiC, it was likely that the crack inside the SiC was caused by thermal stress while crack on the edge was caused by arcing. Although there is a hypothesis that the thermal stress caused crack may happen prior to arcing or between  $0.44 \text{ W}/\text{mm}^2$  and  $0.64 \text{ W}/\text{mm}^2$ , there is confidence that the SiC HOM absorber's limit power flux is above  $0.44 \text{ W}/\text{mm}^2$  because no damage was found during visual inspection at this level. Thus, for the EIC ESR SRF cavity HOM damper, it was determined to use the 240 mm long SBLA, which has a power flux of  $0.34 \text{ W}/\text{mm}^2$ , providing  $> 30\%$  of margin.

## VI. Summary and Plan for EIC HOM damper

HOM damping is crucial for the EIC ESR SRF systems due to the high beam current operating scenarios. A cylindrical shell shape SiC BLA was chosen for the EIC HOM damper. To test the feasibility of the SiC HOM damper, an HOM damper prototype was manufactured and tested. After the HOM absorber assembly was manufactured successfully, an outgassing test was carried out and was demonstrated to satisfy the SRF cavity application. The high-power test results found the power flux limit ( $> 0.44 \text{ W}/\text{mm}^2$ ) to be at least two times higher than what was expected ( $0.2 \text{ W}/\text{mm}^2$ ). These results showed that the LBLA design for a power flux of  $0.19 \text{ W}/\text{mm}^2$  has  $> 100\%$  of margin, and the SBLA design for a power flux of  $0.34 \text{ W}/\text{mm}^2$  has  $> 30\%$  of margin.

More testing will be carried out in the future to continue to characterize the SiC BLA power flux and other properties. All the HOM absorbers for EIC SRF cavities will go through high power test, prior to the installation to the EIC SRF cryomodules.

## ACKNOWLEDGEMENT

The work is supported by Brookhaven Science Associates, LLC under contract No. DE-AC02-98CH10886 with the US DOE. Special Thanks to BNL Laboratory Directed Research and Development (LDRD) program for supporting the HOM prototype manufacture.

The author would like to thank Philipp Kolb (TRIUMF), Michael Kelly (ANL) and Sanghoon Kim (FRIB) for their informative discussion on SiC HOM damper.

## REFERENCES

- [1] EIC Concept Design Report, [https://www.bnl.gov/ec/files/EIC\\_CDR\\_Final.pdf](https://www.bnl.gov/ec/files/EIC_CDR_Final.pdf)
- [2] RHIC, <https://www.bnl.gov/rhic/>
- [3] M. Nishiwaki, K. Akai, T. Furuya, A. Kabe, S. Mitsunobu, Y. Morita, “Developments of HOM dampers for Super KEKB Superconducting cavity”, Proceedings of SRF2013, Paris, France, THP061. <https://epaper.kek.jp/SRF2013/papers/thp061.pdf>
- [4] S. Kim, “HOM Damping in Superconducting Harmonic Cavity for Advanced Photon Source Upgrade”, presented at HOMSC’16, Warnemünde, Germany, 2016. <https://indico.cern.ch/event/465683/>
- [5] R. Eichhorn, J. Conway, Y. He, Y. Li, G. Hoffstaetter, M. Liepe, T. Gruber, M. Tigner, T. O’Connell, P. Quigley, J. Sears, E. Smith, V.D. Shemelin, Higher Order Mode Absorbers for High Current SRF Applications, Proceedings of SRF2015, Whistler, BC Canada, 2015. <https://accelconf.web.cern.ch/srf2015/papers/thba05.pdf>
- [6] P. Kolb, R. E. Laxdal, Y. Ma, Z. Yao, V. Zvyagintsev, “HOM Measurements on the ARIEL eLINAC cryomodules”, Proc of the 2015 Conf on SRF, Whistler, BC, (2015).
- [7] R. Eichhorn, private communications.
- [8] J. Guo, R. Rimmer, G. Park, H. Wang, J. Henry, J. Matalевич, E. Daly, S. Wang, W. Xu, D. Holmes, A. Zaltsman, K. Smith, “Design and Prototyping of the Electron Ion Collider Electron Storage Ring SRF cavity”, 21st International Conference on Radio-Frequency Superconductivity (SRF 2023), Jun. 22-29, 2023.
- [9] J. Guo, R. Rimmer, G. Park, H. Wang, J. Henry, J. Matalевич, E. Daly, S. Wang, W. Xu, D. Holmes, A. Zaltsman, K. Smith, “Design of the Electron Ion Collider Electron Storage Ring SRF cavity”, presented at IPAC’22, Bangkok, Thailand, Jun. 2022, TUPOTK040